Electronic Transport Transition of Hydrogenated Amorphous Silicon Irradiated With Self Ions

Shin-ichiro Sato and Takeshi Ohshima

***Abstract*—Electric conductivity variations of hydrogenated amorphous silicon due to self-ion irradiation, i.e. irradiation with Si or H ions, are comprehensively investigated. The anomalous enhancement of dark conductivity (DC) and photoconductivity (PC) are firstly observed due to proton irradiation in the cases of undoped and n-type a-Si:Hs, and after that both decrease with increasing the irradiation fluence. However, Si ion irradiation does not induce the anomalous enhancement and induce a monotonic decrease in DC and PC in the low fluence regime. It is shown from the Seebeck effect analysis that the anomalous enhancement is caused by generation of donor-centers which have metastable nature at room temperature. The decrease in DC and PC is ascribed to the carrier removal effect and the carrier lifetime decrease accompanied by accumulation of dangling bonds, respectively. However, further irradiation causes the loss of photoconduction and the drastic increase in DC. This indicates that the dominant conduction mechanism changes from the band transport to the hopping transport due to excessive accumulation of dangling bonds. The change in the dominant conduction mechanism occurs at above about 10^{-4} dpa (displacement per atom) and is independent of the majority carrier concentration before irradiation. It is concluded that the conductivity variations caused by self-ion irradiation can be systematically categorized according to the ratio of the nuclear energy deposition to the electronic energy deposition of incident ions.**

***Index Terms*—Amorphous semiconductors, ion radiation effects, photoconducting materials, semiconductivity.**

I. Introduction

WITH the development of high energy physics and space technologies, semiconductor devices used in accelerator facilities and space satellites are required to have high radiation tolerance. Radiation effects on many kinds of semiconductor materials have been extensively studied for the sake of the research and development of radiation-hardened semiconductor devices [1], [2]. Since hydrogenated amorphous silicon (a-Si:H), which are used as a material for photoelectric devices, are known to have high radiation tolerance [3], a-Si:H devices (e.g. photo detectors, particle detectors, and space solar cells) are expected to be utilized in severe radiation environments [4], [5]. With respect to radiation effects on electrical properties of a-Si:H, the electron irradiation studies based on the comparison with the Staebler-Wronski (SW) effect have been mainly performed for decades [6]–[9].

Manuscript received November 29, 2012; revised March 18, 2013; accepted April 29, 2013. Date of publication May 31, 2013; date of current version June 12, 2013.

The authors are with Japan Atomic Energy Agency, Takasaki, 370-1292, Japan (e-mail: sato.shinichiro@jaea.go.jp; ohshima.takeshi20@jaea.go.jp).

Digital Object Identifier 10.1109/TNS.2013.2261320

In addition to this, studies on self-ion irradiation effects, i.e. silicon (Si) ion and proton irradiation effects, are also crucial for the application of a-Si:H devices in neutron fields such as plasma observation equipments for fusion reactors and photo-sensors in nuclear power plants [5]. Since space solar cells degrade due to exposure of electrons and protons, knowledge about the electron irradiation effects as well as the proton irradiation effects are especially important for the application to space thin film a-Si solar cells [10]. In spite of these facts, self-ion irradiation effects on electrical properties of a-Si:H are still unclear and only a few reports have been published. For instance, Coffa *et al.* have reported that electric conductivity of a-Si:H thin films increased with increasing a fluence of 2.0 MeV Si ions because of the enhancement of the hopping transport due to accumulation of radiation defects [11]. On the other hand, Kishimoto *et al.* have reported that the electric conductivity increased about two orders of magnitude due to 17 MeV proton irradiation and have concluded that this phenomenon was caused by the formation of shallow electronic states based on the electronic excitation effect of incident protons [12]. They have also discussed the metastable balance between formation and annihilation of the electronic states, indicating that the conductivity variation was not determined by a simple accumulation of deep-level radiation defects. Both results cannot be simply ascribed to the same phenomena when taking into account the fact that 2.0 MeV Si ions and 17 MeV protons have much different ratio of nuclear and electronic energy depositions (stopping powers), and also a consistent interpretation of the increase in conductivity has not been obtained by both research groups.

Generally, radiation defects in semiconductors hinder the band conduction which is the main mechanism of electric conduction. This is because the radiation defects generate localized levels in the bandgap and they act as carrier recombination centers [13]. This results in the decrease in carrier lifetime and photoconductivity (PC). The majority carrier concentration and the dark conductivity (DC) also decrease when the radiation defects compensate donor or acceptor levels as deep-levels [14]. Hence, it is obvious that the results of self-ion irradiation reported from Coffa *et al.* and Kishimoto *et al.* cannot be explained by such a general interpretation of radiation effects on semiconductors only. However, if the radiation defects act as donor or acceptor levels, the value of DC does not always decrease monotonically. For example, ion irradiation converts germanium semiconductors from n- to p-type [15] and the Czochralski-grown Si, which has relatively high oxygen impurities, from p- to n-type [16]. Furthermore, when the radiation defects accumulate excessively due to high dose irradiation,

0018-9499/$31.00 © 2013 IEEE

TABLE I
TYPICAL CHARACTERISTICS OF SAMPLES

Sample	Thickness (μm)	H Concentration (at.%)	DC (S/cm)	PC (S/cm)
Undoped	0.30	11.6	4.0×10^{-11}	9.3×10^{-6}
n-Type (P doped)	0.27	13.5	3.7×10^{-3}	1.0×10^{-3}
p-Type (B doped)	0.21	15.7	2.2×10^{-6}	3.9×10^{-6}

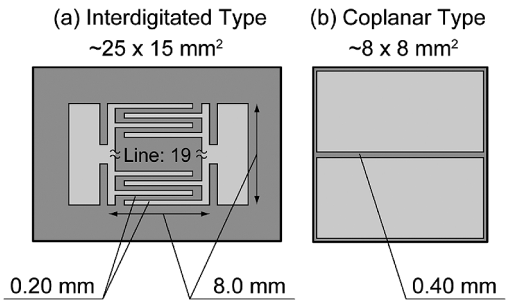

Fig. 1. A schematic drawing of the sample structure used for (a) conductivity measurement and (b) thermoelectric power measurement. Light gray areas represent the aluminum electrodes. (a) Interdigitated type; (b) coplanar type.

the drastic increase in the density of states in the bandgap may result in a loss of the band conduction. The conductivity variation of a-Si:H due to irradiation is determined by what kinds of levels the accumulated radiation defects act as. Therefore, variations of the semiconductor properties in a wide range of irradiation fluence should be clarified in order to elucidate the role of radiation defects. It is also necessary for practical use of radiation-hardened a-Si:H devices to understand the variation of the electric conductivity in radiation environments.

Against this background, we have investigated DC and PC variations of a-Si:H thin films irradiated with energetic ions and revealed the fluence dependence for undoped a-Si:H [17] and for doped (n-type and p-type) a-Si:H [18]. Variations of PC of undoped a-Si:H irradiated with protons as well as the thermal stability and the temperature dependence were clarified in [19]. In addition, the mechanism of radiation-induced conductivity (RIC) in undoped and n-type a-Si:Hs was elucidated in [20]. However, these previous works have focused on the ion irradiation effects in the fluence regime less than 10^{-4} dpa (displacement per atom). In this study, the fluence range to be investigated is extended to 1 dpa and the electric transport transition from the band transport to the hopping transport is found. In order to investigate the variations of DC, PC, and thermoelectric power (Seebeck coefficient) due to self-ion irradiation, *in-situ* measurement techniques are used. *In-situ* techniques are very useful for investigating variations in a wide range of irradiation fluence continuously and relaxation phenomena of the radiation effects. Metastability of the radiation effects after irradiation is also discussed. Moreover, the relations among the electric property variation, the hydrogen concentration variation, and the hydrogen bonding state variation are discussed from the results of infrared absorption spectroscopy. As a result, including the previously obtained results, a comprehensive and systematic interpretation of electric conductivity variations of a-Si:H films due to self-ion irradiation are successfully obtained in the very wide fluence range from 10^{-10} dpa to 1 dpa. This interpretation can be applied to both undoped and doped a-Si:Hs. In addition, the physical application limit for a-Si:H photoelectric devices is clarified by analyzing the photosensitivity variations due to self-ion irradiation.

II. EXPERIMENTAL

The samples used in this study were device-grade undoped, n-type (phosphorous doped) and p-type (boron doped) a-Si:H thin films fabricated on glass substrates by plasma enhanced chemical vapor deposition (PECVD) at the National Institute of Advanced Industrial Science and Technology (AIST). The excitation frequency was 13.56 MHz. The substrate temperature during deposition and the gas flow rates were 180°C and $SiH_4/H_2 = 20/100$ sccm for undoped samples, 195°C and $SiH_4/H_2/PH_3 = 20/80/23$ sccm for n-type samples, and 200°C and $SiH_4/H_2/B_2H_6 = 10/100/30$ sccm for p-type samples, respectively (PH_3 and B_2H_6 are 5,000 ppm mixtures with hydrogen balance gas). The sample structure is shown in Fig. 1. Interdigitated type and coplanar type aluminum Ohmic electrodes were formed on the samples for conductivity measurement and for thermoelectric power measurement, respectively. All the samples were previously light-soaked using a metal halide lamp to stabilize their electrical properties. The sample thicknesses, the hydrogen concentration, and the conductivity are listed in Table I.

The samples were irradiated with 10 MeV and 0.10 MeV protons, and 2.8 MeV Si ions at room temperature (RT) and their conductivity variation as a function of irradiation fluence was investigated *in-situ* in an irradiation vacuum chamber. The Seebeck coefficient variation due to 0.10 MeV proton irradiation was also investigated *in-situ*. Ion irradiation was performed at the Takasaki Ion Accelerators of advanced Radiation Application (TIARA), Japan Atomic Energy Agency (JAEA). A raster beam scanning system was used for uniform irradiation of the whole area of a sample. The fluctuation of beam uniformity was estimated to be within ±5%. The projected ranges of all the ions are larger than thickness of the a-Si:H film and deposit their energy almost uniformly through the film, according to the Monte Carlo simulation code, TRIM [21]. Thus, no passivation by the implanted hydrogen atoms of dangling bonds in the a-Si:H films is expected. In the TRIM calculation, 2.3 $\mathrm{g/cm^3}$ mass density and 11.6% hydrogen concentration were used for the undoped a-Si:H. These values were experimentally determined by using Rutherford backscattering spectroscopy (RBS) and elastic recoil detection analysis (ERDA). The default values of displacement energy installed in TRIM were used: 15 eV for Si and 10 eV for H. Electronic energy deposition (S_e), nuclear energy deposition (S_n), $S_\mathrm{n}/S_\mathrm{e}$, fluence per unit dpa (ϕ_dpa), and projected range (R) of ions in the undoped a-Si:H are listed in Table II.

TABLE II
TRIM CALCULATION RESULTS FOR UNDOPED SAMPLE

Ion	Energy (MeV)	S_e (eV/nm)	S_n (eV/nm)	S_n/S_e	ϕ_{dpa} (cm^{-2})	R (μm)
Proton	10	7.4	1.5×10^{-3}	2.1×10^{-4}	4.6×10^{20}	6.6×10^{2}
	0.10	1.1×10^{2}	0.16	1.5×10^{-3}	4.5×10^{18}	0.89
Silicon	2.8	2.0×10^{3}	40	2.0×10^{-2}	9.8×10^{15}	2.2
	0.38	5.1×10^{2}	2.0×10^{2}	0.39	9.8×10^{14}	0.53

Values of S_e, S_n and ϕ_{dpa} are average values along the depth direction. The same values were also applied for the analysis of the n-type and p-type a-Si:Hs. Note that the displacement energy in a-Si:H may be different from that in crystalline Si (c-Si) and the values listed in Table II vary depending on the displacement energy [22]. However, this effect is sufficiently small and does not affect the discussion and the conclusions in this study.

The current-voltage $(I - V)$ characteristics of the samples were measured *in-situ* in the irradiation chamber. *In-situ* $I - V$ measurement was performed under dark conditions for DC and under light illumination for PC. The light spectrum and intensity were AM-0 (Air Mass zero) and 136.7 mW/cm^2 (1 sun), respectively. The light fluctuation was estimated to be within ±0.5%. Hereinafter, DC is defined as the conductivity measured under dark conditions and PC is defined as the difference between the DC and the conductivity under light illumination. The voltage sweep range was from −10.0 V to +40.0 V (from −0.500 to +2.00 kV/cm) and the conductivity was derived from the slope of $I - V$ characteristics. Ion beams were stopped by a shutter during measurement and the irradiation was resumed after completion of the measurement. Details of the experimental setup are described in [19].

The variation of majority carrier concentration due to ion irradiation can be clarified by analyzing variations of both the electric conductivity and the Seebeck coefficient. The *in-situ* thermoelectric power measurement system was installed in the irradiation chamber to investigate the Seebeck coefficient variations of the undoped and n-type a-Si:Hs due to 0.10 MeV proton irradiation. The Seebeck coefficient was derived from the ratio of the thermoelectric power divided by the temperature difference. The temperature difference was around 20 K. The electric potential difference (thermoelectric power) between the electrodes and the temperature difference were measured by an electrometer and K-type thermocouples, respectively. The proton beams were stopped by a shutter during measurement and the irradiation was resumed after completion of the measurement. Details of the experimental procedure are described in [22].

III. RESULTS

A. DC and PC Variations Due to Self-Ion Irradiation

Fig. 2 shows typical $I - V$ characteristics before and after self-ion irradiation. When the conductivity was very high, the voltage sweep range was limited to less than 40.0 V because of a current compliance in the measurement system (see the dotted line in Fig. 2(b)). Almost linear $I - V$ characteristics were obtained in most cases, indicating that a good Ohmic contact was formed. In particular, almost linear $I-V$ characteristics

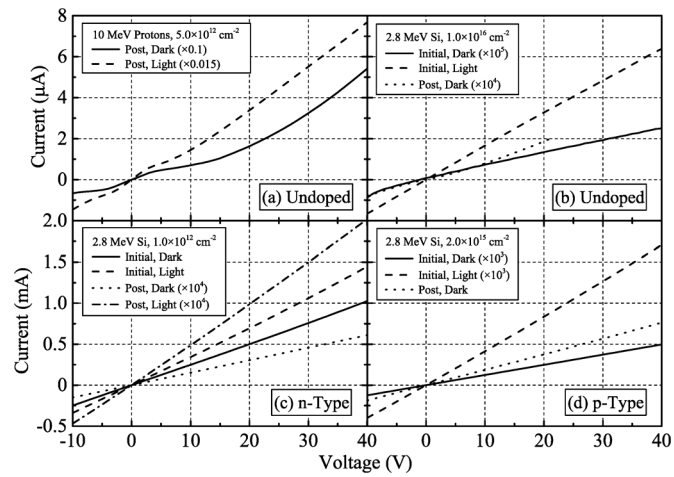

Fig. 2. Typical $I - V$ characteristics before and after self-ion irradiation: (a) the undoped a-Si:H irradiated with 10 MeV protons at 5.0×10^{12} cm^{-2}, (b) the undoped a-Si:H irradiated with 2.8 MeV Si ions at 1.0×10^{16} cm^{-2}, (c) the n-type a-Si:H irradiated with 2.8 MeV Si ions at 1.0×10^{12} cm^{-2}, and (d) the p-type a-Si:H irradiated with 2.8 MeV Si ions at 2.0×10^{15} cm^{-2}. Note that the ordinate axes are multiplied in order to show the data properly.

were always obtained in the case of doped a-Si:H. In contrast, super-Ohmic (convex downward) $I - V$ characteristics were sometimes obtained in the undoped a-Si:H, which are shown as examples in Fig. 2(a). Such a convex downward shape was seen when the conductivity was drastically increased due to 10 MeV proton irradiation, although it was not necessary to be considered. Here, it should be noted that the electric conductivity of a-Si:H depends on electric field and the field-enhanced conductivity is observed under high electric field (usually around 10^2 kV/cm) [23]–[25]. Although the applied electric field in this study was sufficiently lower than that (less than 2.00 kV/cm), radiation effects on the electric-field dependence are unclear and the super-Ohmic shape observed in Fig. 2(a) may result from it. However, the effects contribute little to the obtained results. In all cases, the approximate line was derived from the obtained $I-V$ characteristics by the least squares approximation and the conductivity (DC and DC+PC) was calculated from the slope of the line.

Fig. 3 shows DC and PC variations of the undoped a-Si:H irradiated with 10 MeV protons. A unit of fluence (cm^{-2}) can be converted into a unit of dpa and the abscissa axis in the upper part is scaled by dpa. The PC value, which was 7.3×10^{-6} S/cm before irradiation, increased with increasing the irradiation fluence and reached a maximum of 1.1×10^{-3} S/cm at the fluence of 1.0×10^{13} cm^{-2}. However, the decrease in PC was observed at above 1.0×10^{13} cm^{-2} and the PC value at above

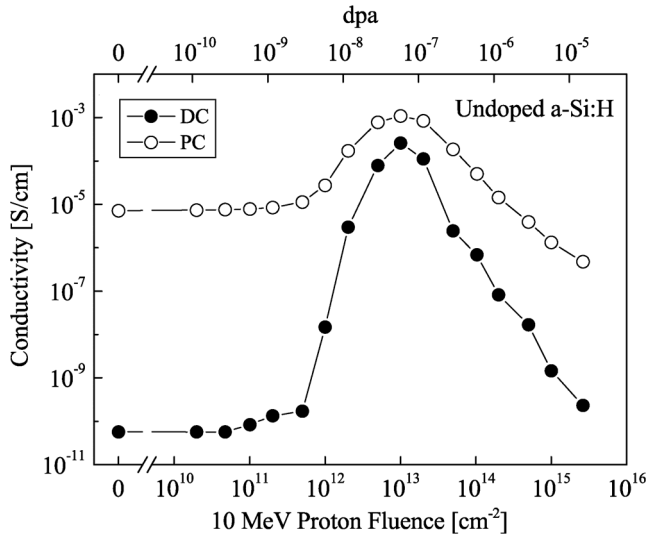

Fig. 3. Dark conductivity (DC) and photoconductivity (PC) variations of the undoped a-Si:H due to 10 MeV proton irradiation at room temperature (RT). The abscissa axis in the upper part is converted from fluence to a unit of displacement per atom (dpa). The same is true in Figs. 4, 5, 14, and 15.

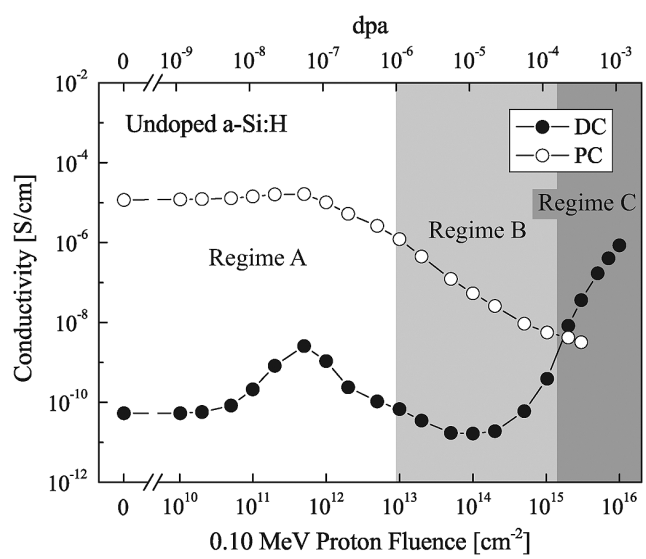

Fig. 4. DC and PC variations of the undoped a-Si:H due to 0.10 MeV proton irradiation at RT.

5.0×10^{14} cm^{-2} became smaller than the value before irradiation. The DC value varied more drastically due to irradiation. The DC value, which was 5.7×10^{-11} S/cm before irradiation, increased with increasing the fluence and reached a maximum of 2.6×10^{-4} S/cm at 1.0×10^{13} cm^{-2}. The peak fluence corresponded to that of PC. The DC value decreased with increasing the fluence above 1.0×10^{13} cm^{-2}. In general, both the DC and PC for semiconductor materials decreased due to radiation, which is discussed in Section IV-A. Hereinafter, the increase in both DC and PC observed in the low fluence regime is called anomalous conductivity enhancement.

Fig. 4 shows DC and PC variations of the undoped a-Si:H irradiated with 0.10 MeV protons. The anomalous conductivity enhancement was also observed in the case of 0.10 MeV proton irradiation. Both the DC and PC values had a peak at the fluence

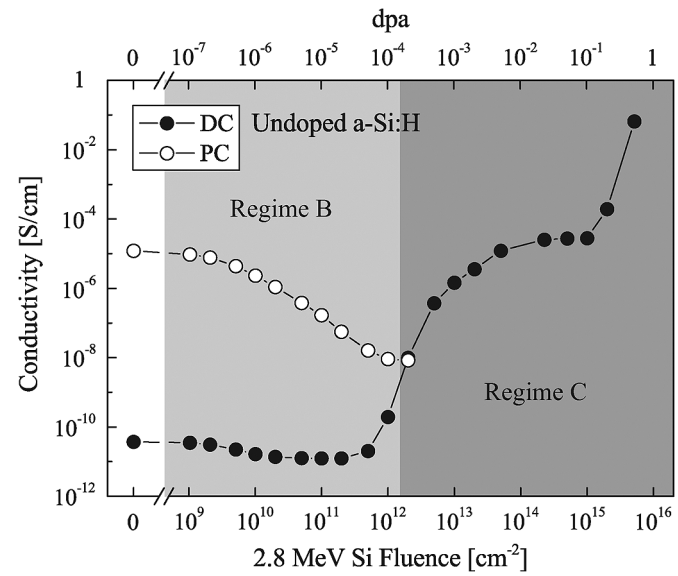

Fig. 5. DC and PC variations of the undoped a-Si:H due to 2.8 MeV Si ion irradiation at RT.

of 5.0×10^{11} cm^{-2} and after that decreased with increasing the fluence (Regime A). However, the increase in DC was observed again at above the fluence of 1.0×10^{14} cm^{-2}, whereas the PC continued to decrease (Regime B). Eventually the DC became larger than the PC at the fluence of 2.0×10^{15} cm^{-2}. The DC continued to increase with increasing the fluence and no photoconduction was observed in this fluence regime (Regime C). In other words, deriving from the difference between the DC and the conductivity under light illumination (DC+PC), the PC value could not be found when the difference was negligibly small. Hereinafter, the fluence regimes A, B, and C are occasionally represented as the low, middle, and high fluence regimes, respectively.

The DC and PC variations of the undoped a-Si:H due to 2.8 MeV Si ion irradiation are shown in Fig. 5. In this case, the anomalous conductivity enhancement was not observed in the low fluence regime and the decrease in DC and PC appeared up to the fluence of 2.0×10^{11} cm^{-2} (Regime B). The increase in DC was observed at above this fluence whereas the PC decreased. The photoconduction was eventually lost at above 2.0×10^{12} cm^{-2} (Regime C).

B. DC and PC Variations Immediately After Irradiation

Both the anomalous conductivity enhancement in the low fluence regime and the increase in DC in the high fluence regime gradually decayed with time at RT. Time decay of the anomalous conductivity enhancement is depicted in Fig. 6. Both the DC and PC values of the undoped a-Si:H were measured periodically in the irradiation chamber after irradiation with 10 MeV protons of 1.5×10^{13} cm^{-2}. As a result, both conductivities decreased exponentially with time, retaining higher values than the values before irradiation. Fig. 7 shows the DC decay with time of the undoped a-Si:H after irradiation with 0.10 MeV protons of 1.0×10^{16} cm^{-2}. As is the case with Fig. 6, the DC decreased exponentially with time, retaining a higher value than the value

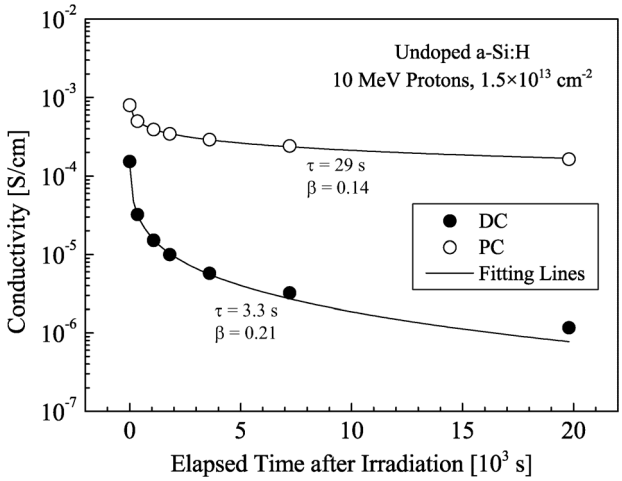

Fig. 6. Time decay of DC and PC values of the undoped a-Si:H irradiated with 10 MeV protons at the fluence of 1.5×10^{13} cm^{-2} at RT. Solid lines are the fitting lines using (1).

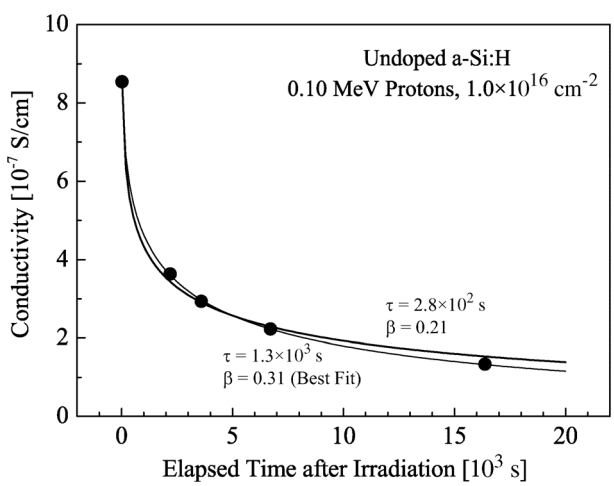

Fig. 7. DC variation with time in the undoped a-Si:H irradiated with 0.10 MeV protons at the fluence of 1.0×10^{16} cm^{-2} at RT. The solid line is the fitting line using (1) and the bold line is the fitting line when β is regarded as a constant value of 0.21.

before irradiation. Also, no photoconduction was found in this time region.

The conductivity variation of a-Si:H with time are known to be represented as the stretched exponential model [26]:

$$\sigma \propto \exp\left[-\left(\frac{t}{\tau}\right)^{\beta}\right] \tag{1}$$

where σ, t, and τ denote the conductivity (S), the elapsed time after irradiation (s), and the time constant (s), respectively. β is the power index which is a value from 0 to 1. Both the anomalous conductivity enhancement and the increase in DC in the high fluence regime could be fitted by (1), although no physical meaning was included in the value of β. The fitting results are shown in Figs. 6 and 7. Values of the parameters: τ and β are also shown in the figures. However, the value of β should be equivalent in order to compare the time constant. The bold line in Fig. 7 represents a fitting result when the value of β was 0.21, which was equivalent to that in Fig. 6. When comparing the time constant (τ), the time decay of the anomalous DC enhancement

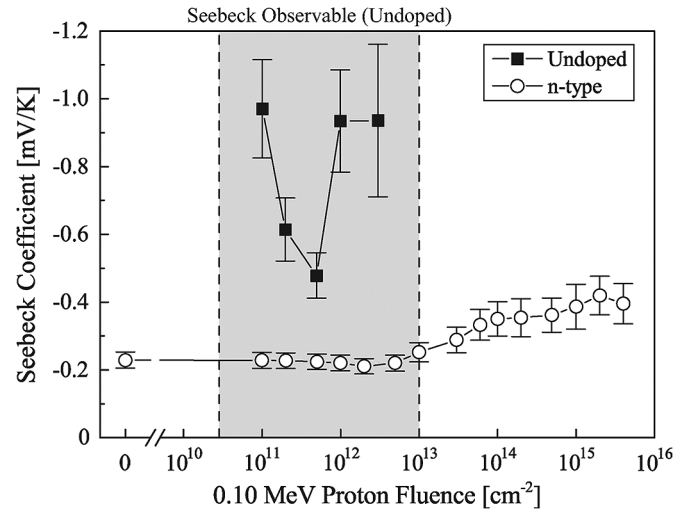

Fig. 8. Seebeck coefficient variations of the undoped (closed squares) and n-type (open circles) a-Si:Hs due to 0.10 MeV proton irradiation at RT. The shaded zone represents the fluence regime in which the Seebeck effect was observable in the undoped a-Si:H.

(3.3 s) was about two orders lower than that of the increased DC in the high fluence regime (2.8×10^2 s). This indicates that the anomalous DC enhancement decayed more rapidly than the increased DC in the high fluence regime, and thus, their DC increases are based on different origins.

C. Seebeck Coefficient Variation Due to Proton Irradiation

Fig. 8 shows the Seebeck coefficient variations of the undoped and n-type a-Si:Hs irradiated with 0.10 MeV protons. No Seebeck effect was observed in the undoped a-Si:H without irradiation and also after the irradiation of 3.0×10^{10} cm^{-2}. However, the Seebeck coefficient of -0.97 mV/K was observed after the irradiation of 1.0×10^{11} cm^{-2}. The Seebeck coefficient reached a maximum (-0.48 mV/K) at 5.0×10^{11} cm^{-2}. The negative Seebeck effect was observed up to the fluence of 3.0×10^{12} cm^{-2}. The Seebeck effect could not be observed again at above 1.0×10^{13} cm^{-2} because of high noise, which was due to low conductivity of the sample. The Seebeck effect could be observed in the fluence regime in which the anomalous conductivity enhancement was observed (see Fig. 4). The Seebeck coefficient of the n-type a-Si:H which was -0.23 mV/K before irradiation slightly increased up to the fluence of 2.0×10^{12} cm^{-2} and after that decreased with increasing the fluence. The Seebeck coefficient was -0.42 mV/K at the fluence of 2.0×10^{15} cm^{-2}. As the variations of the Seebeck coefficient due to irradiation are thought to be mainly attributable to the variations of majority carrier concentration, they are correlated with the conductivity variations.

IV. Discussion

A. Electronic Transport Transition From Band Conduction to Hopping Conduction

In this section, we clarify the mechanism of PC and DC variations due to self-ion irradiation. First of all, a general interpretation of conductivity variations of semiconductor materials exposed to radiations is briefly mentioned. Subsequently, the mechanism of the PC and DC variations of a-Si:H is discussed.

DC and PC of semiconductors, σ_{d} and σ_{p} are represented as follows:

$$\sigma_{\mathrm{d}} = e\mu n \tag{2}$$

$$\sigma_{\mathrm{p}} = e\mu\Delta n = e\mu\tau_{\mathrm{L}}G \tag{3}$$

where e is the elementary charge, μ is the majority carrier mobility $(\mathrm{cm}^2/(\mathrm{V}\cdot\mathrm{s}))$, and n denotes the majority carrier concentration (cm^{-3}). Also, Δn, τ_{L}, and G denote the photo-excited carrier concentration (cm^{-3}), the carrier lifetime (s), and the carrier generation ratio $(\mathrm{cm}^{-3}\cdot\mathrm{s}^{-1})$, respectively. In the case of undoped a-Si:H, the electron mobility is sufficiently larger than the hole mobility and (3) is always applicable although the dependence of PC with the carrier generation ratio (G) generally depends on the excitation intensity [21].

Next, variations of DC and PC of semiconductor materials due to radiations are considered. When exposed to radiations, structural disorders such as atomic displacement and defect creation are produced in semiconductor materials because of the displacement damage effect. Radiation defects act as a carrier recombination center and provide a decrease in carrier lifetime (τ_{L}). They create deep levels near the intrinsic Fermi level and also may provide a decrease in majority carrier concentration (n) of impurity-doped semiconductors by compensating the donor or acceptor levels. This is called the carrier removal effect [27]. Since the carrier scattering mechanism does not change in the low fluence regime (e.g. less than 5×10^{-6} dpa in the case of c-Si [14]), the carrier mobility (μ) is considered as a constant. The carrier generation ratio (G) can also be considered unchanged for radiation exposure. Hence, the decrease in PC and DC is mainly provided by the carrier lifetime decrease and the carrier removal effect, respectively.

As shown in Figs. 3 and 4, the anomalous conductivity enhancement in the low fluence regime was observed in the case of 10 MeV and 0.10 MeV proton irradiations. This cannot be explained by the carrier lifetime decrease and the carrier removal effect, and thus a different mechanism should be considered. The proton-irradiated undoped a-Si:H showed the negative Seebeck effect only in the low fluence regime, as shown in Fig. 8. The Seebeck coefficient of an n-type semiconductor is negative and a p-type is positive. The fact of emergence of the negative Seebeck effect suggests that the conduction type of undoped a-Si:H was n-type in its fluence regime. Since the DC increases with increasing the donor concentration, the increase in DC is attributed to the generation of donor-centers due to proton irradiation. Also, the PC of n-type a-Si:H is higher than that of intrinsic one, and thus the increase in PC occurs with the increase in DC [28]. However, the generated donor-centers decrease or are compensated with time at RT, which are clarified in Fig. 6. These metastable phenomena could be clearly detected by using *in-situ* measurement techniques.

Fig. 9 shows the DC, PC, and Seebeck coefficient variations as a function of the electronic energy deposition density. The electronic energy deposition density $(\mathrm{eV/cm}^3)$ is defined as the product of the electronic energy deposition (eV/cm) and the fluence of incident radiation (cm^{-2}). As a result, the fluence regime in which the anomalous conductivity enhancement was observed was in accordance with that in which the negative Seebeck effect was observed. This result strongly suggests that the

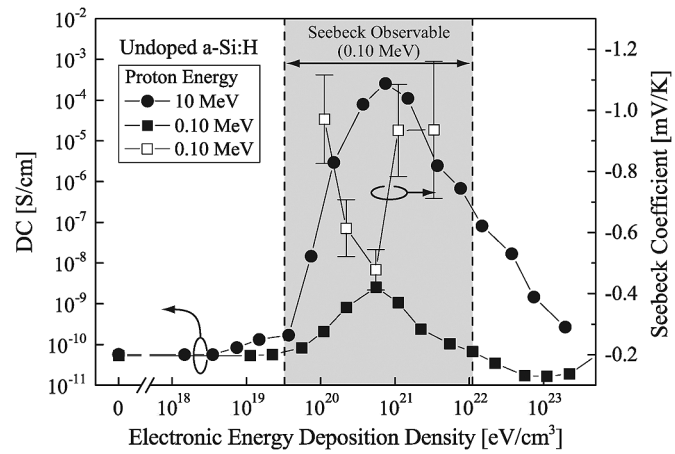

Fig. 9. DC variations (closed symbols) and Seebeck coefficient variation (open squares) of the undoped a-Si:H as a function of electronic energy deposition density from protons. The left ordinate axis represents the DC value and the right ordinate axis represents the Seebeck coefficient.

donor-center generation, which causes the increase in DC and PC, is associated with the electronic excitation effect of incident protons. The relationship between the energy deposition process and the anomalous conductivity enhancement is described in detail elsewhere [17].

On the other hand, the DC and PC values of undoped a-Si:H which increased in the low fluence regime decreased with further irradiation. The decrease in DC and PC observed in the middle fluence regime is thought to be due to the carrier removal effect and the decrease in carrier lifetime accompanied by the accumulation of radiation defects which produce deep-levels, respectively. Well known radiation defects in a-Si:H are dangling bonds and several previous studies have reported that the dangling bond density increased from 10^{16} cm^{-3} to above 10^{18} cm^{-3} due to radiation exposure [29]. In the middle fluence regime, the generated donor-centers were compensated by the dangling bonds or disappeared by some effects of further irradiation [22], and the dangling bonds were exclusively accumulated with increasing the fluence. The decrease in Seebeck coefficient of n-type a-Si:H in the fluence regime between 10^{13} cm^{-2} and 10^{15} cm^{-2} is also attributed to the carrier removal effect, which causes the decrease in majority carrier concentration. In fact, the DC of n-type a-Si:H decreased due to 0.10 MeV proton irradiation in this fluence regime. It was shown in our previous work that the majority carrier concentration decreased due to irradiation, whereas the carrier mobility did not change according to the Hall measurement [18]. However, the increase in DC was observed again at the fluence above 1.0×10^{14} cm^{-2} in Fig. 4 and above 2.0×10^{11} cm^{-2} in Fig. 5, whereas the PC continued to decrease and became negligibly small at above 2.0×10^{15} cm^{-2} in Fig. 4 and at above 2.0×10^{12} cm^{-2} in Fig. 5. This is because the dangling bonds which are excessively accumulated do not necessarily simply provide the deep-levels. The reason is explained as follows.

The electric conduction in a-Si:H is dominated by the transport of thermally excited carriers near the mobility edge (band transport). Deep-level defects act as localized states and interrupt the band transport. However, when radiation defects are excessively accumulated due to irradiation and the density of lo-

calized states increases, a number of electrons which occupy the localized states increases whereas a number of electrons which cross over the mobility edge of the extended states decreases. The former electrons contribute to the electric conduction by hopping between the localized states. This is called the hopping conduction. For instance, the electric conduction of a-Si:H at low temperature is dominated by the hopping transport, since the number of the latter electrons decreases and the number of the former electrons becomes relatively large at low temperature [30]. Also, the hopping conduction is dominant in hydrogen-free amorphous silicon (a-Si) at RT, in which the dangling bond density is usually around 10^{20} cm^{-3} [31]. In that case, the number of the former electrons is much larger than that of the latter one and thus the contribution of the band conduction is relatively small. It would appear that a similar situation occurred in the ion-irradiated a-Si:H in the high fluence regime (e.g. above 1.0×10^{14} cm^{-2} in Fig. 4 and above 2.0×10^{11} cm^{-2} in Fig. 5). Namely, the increase in DC and the disappearance of photoconduction strongly indicate that the band conduction was lost and the hopping conduction became dominant due to the excessive accumulation of dangling bonds: In other words, the change in dominant electric conduction mechanism from the band transport to the hopping transport occurred in the high fluence regime. Carriers excited by light illumination do not transport the mobility edge and little photoconduction occurs when the hopping conduction is dominant. The PC decreases with increasing fluence and becomes negligibly small in the high fluence regime, whereas the DC increases due to the increase in the hopping transport. However, the excessively accumulated dangling bonds can be annealed at RT and the DC based on the hopping conduction gradually decrease with time, which are shown in Fig. 7. Unfortunately, the microscopic nature of excessively accumulated dangling bonds is not clear despite that studies on photothermal deflection spectroscopy (PDS) and electron spin resonance (ESR) have been performed in order to investigate the detail of radiation defects in a-Si:H [6], [32]. The monotonic increase in dangling bonds and no unique spectrum originating from the radiation defects have been found at present. However, it is known to be relatively stable dangling bonds which are different from the light-induced dangling bonds [33]. We have also observed the stable dangling bonds which were never thermally annealed. The undoped a-Si:H irradiated with 0.10 MeV protons at 1.0×10^{15} cm^{-2} was annealed at 423 K for 4 hours in nitrogen atmosphere, and as a result, the value of PC only recovered to 7% of the initial value. Consequently, there are at least two kinds of dangling bonds in the irradiated a-Si:H. One is the reversible dangling bonds which are the same one generated by light-illumination (the SW effect). The other is the stable dangling bonds which are not thermally annealed and it is unique to radiation irradiation. The decrease in hopping conduction immediately after irradiation, shown in Fig. 7, is thought to be due to the decrease in density of reversible dangling bonds. The difference of stability may originate from bonding states of the neighboring atoms.

Fig. 10 shows DC variations of the undoped, n-type, and p-type a-Si:Hs irradiated with 2.8 MeV Si ions. Variation of DC of the undoped a-Si:H irradiated with 0.10 MeV protons are also shown in Fig. 10. The abscissa axis is converted from fluence to dpa. The DC of the undoped a-Si:H slightly decreased up to around 3×10^{-5} dpa and after that increased dramatically. The DC of the n-type and p-type a-Si:Hs decreased up to around 1×10^{-4} dpa and after that also dramatically increased. It is noteworthy that all the DC variations aligned at above 1×10^{-4} dpa. This means that the DC value at above 1×10^{-4} dpa is independent of the dopant concentration before irradiation and only depends on the dpa value. That is, the donor and acceptor levels are almost completely compensated by the deep-level defects (dangling bonds) in this fluence regime and the hopping conduction increases with accumulating dangling bonds. The fact that the increase in DC based on the enhancement of the hopping conduction could be scaled by a unit of dpa strongly indicates that the accumulation of dangling bonds is attributed to the displacement damage effect of incident ions.

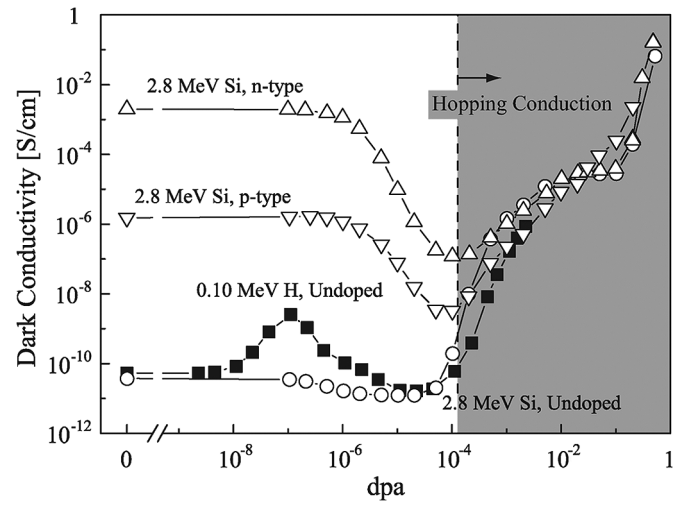

Fig. 10. DC variations of the undoped, n-type and p-type a-Si:Hs due to self-ion irradiation. The abscissa axis is scaled by dpa.

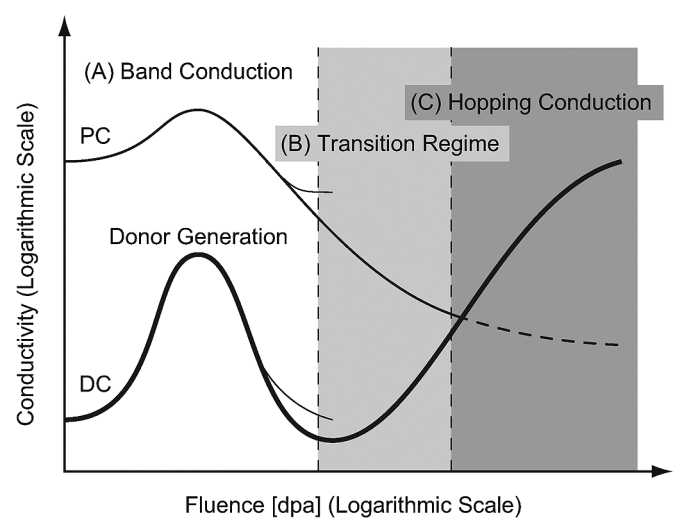

Fig. 11. DC and PC variations of undoped a-Si:H due to irradiation.

The DC and PC variations due to ion irradiation can be systematically categorized according to the ratio of the nuclear energy deposition to the electronic energy deposition (S_n/S_e) of incident ions. Fig. 11 shows a general representation of DC and PC variations of undoped a-Si:H due to irradiation. Firstly, in the case of ions with small S_n/S_e such as 10 MeV protons, the anomalous conductivity enhancement appears in the low

fluence regime whereas the increase in DC and the disappearance of PC are never observed in the high fluence regime. Thus, only the variations in the fluence regime A appear due to irradiation and their conductivity variations are saturated in the high fluence regime (see fine lines in the figure). Since the dangling bond generation process is dominated by the displacement damage effect based on S_{n} and the net dangling bond density is determined by a balance between defect creation ratio of incident ions and thermal annealing of defects, irradiation of ions with small $S_{\mathrm{n}}/S_{\mathrm{e}}$ ratio does not produce a dangling bond density enough to be dominated by the hopping conduction. Accordingly, the dangling bond density is saturated in the regime B. It is believed that this is also applicable in the case of high energy electron irradiation. On the contrary, in the case of ions with large $S_{\mathrm{n}}/S_{\mathrm{e}}$ such as 2.8 MeV Si ions, the anomalous conductivity enhancement is not observed. This is because the conductivity decrease caused by the accumulation of dangling bonds is more dominant than the conductivity enhancement caused by the donor-center generation. Only the decrease in DC and PC is observed up to the middle fluence regime and after that the increase in DC is observed while the photoconduction is lost in the high fluence regime. These variations are simply caused by the accumulation of dangling bonds. Therefore, it is concluded that only the variations in the regimes B and C appear and the variations in the regime A are not observed in the case of ions with large $S_{\mathrm{n}}/S_{\mathrm{e}}$. However, both effects of the donor-centers and the dangling bonds appear in the case of ions with intermediate $S_{\mathrm{n}}/S_{\mathrm{e}}$ between them such as 0.10 MeV protons. Namely, all the variations from the regime A to the regime C (the anomalous conductivity enhancement in the low fluence regime, the decrease in DC and PC in the middle fluence regime, and the increase in DC and the disappearance of PC in the high fluence regime) clearly appear. We anticipate that the conductivity variations of a-Si:H due to any charged particle irradiation follows the principle described here.

Finally, variation of the majority carrier mobility which governs the electric conduction is discussed. Although the mobility variation due to irradiation was not experimentally investigated in this study, it is possible to discuss it qualitatively. As explained earlier, the electric conduction is dominated by the free carriers near the mobility edge and the free carrier mobility hardly changes due to irradiation in the fluence regime A. With enhancing the hopping transport in the fluence regimes B and C, the band transport is undermined mainly because of the carrier removal effect. Since the electric conductivity (DC) governed by the hopping transport is also represented as the product of elementary charge, carrier mobility, and hopping site density, which basically equals to (2). The enhancement of DC is thought to be mainly caused by the increase in hopping site density accompanied by the increase in localized density of states (dangling bonds). However, the hopping mobility has the potential to increase due to irradiation. The hopping mobility, μ_{H} is represented as follows [34]:

$$\mu_{\mathrm{H}} = \frac{eR^2\nu}{6k_{\mathrm{B}}T}\exp\left(-\frac{2R}{a} - \frac{W}{k_{\mathrm{B}}T}\right) \tag{4}$$

where R the average distance among hopping sites, ν the phonon frequency, k_{B} the Boltzmann's constant, T the temperature, a the extension of the electron wavefunction (the localization length), and W the average hopping energy. R, a, and W vary as a function of the energy level of hopping sites $(\varepsilon_{\mathrm{H}})$. With increasing the dangling bonds due to irradiation, the average distance with neighboring dangling bonds decreases, and thus, R decreases. Assuming R is regarded as the variable in (4), μ reaches its peak at $R = a$. It means that the hopping mobility increases with decreasing the average hopping distance because of $a \approx 1$ nm [25] and thus, $R > a$. Therefore, not only the increase in hopping site density, but also the increase in hopping mobility may contribute to the drastic enhancement of DC in the fluence regime C. To explore this point, further study such as time-of-flight (TOF) measurement [35] and the analysis of temperature dependence [23], [36], [37] is required.

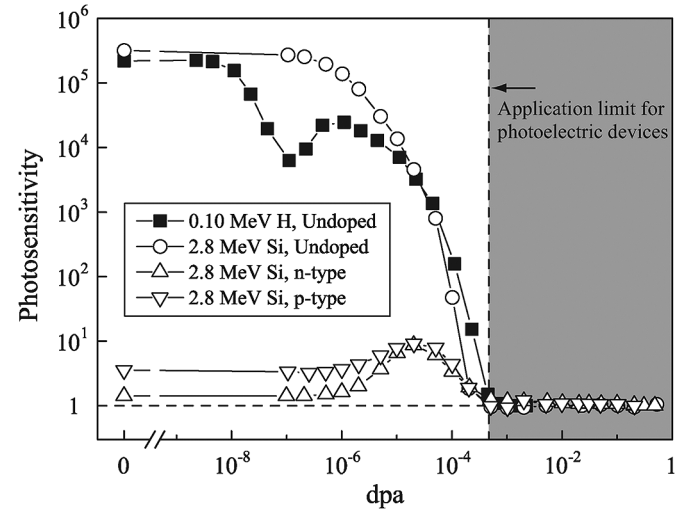

Fig. 12. Photosensitivity variations of the undoped, n-type and p-type a-Si:Hs due to self-ion irradiation. The abscissa axis is scaled by dpa.

B. Application Limit for a-Si:H Photoelectric Devices

One of the most important electric properties for photoelectric devices is the photosensitivity, which is the amplification factor of electric conductivity by light illumination. In this study, the photosensitivity, P is defined as the following equation:

$$P = \frac{(\sigma_{\mathrm{d}} + \sigma_{\mathrm{p}})}{\sigma_{\mathrm{d}}}. \tag{5}$$

Undoped a-Si:H has a high photosensitivity above 10^5. However, both the carrier lifetime and the PC decrease due to the accumulation of radiation defects, and as a result the photosensitivity decreases with increasing ion fluence. Eventually the photosensitivity is close to 1 in the high fluence regime, which means the loss of photoconduction. Since the application limit of a photoelectric device is primarily determined by the photosensitivity degradation, the photoelectric device cannot be applied in such a radiation environment.

Fig. 12 shows photosensitivity variations of the undoped, p-type and n-type a-Si:Hs irradiated with 0.10 MeV protons or 2.8 MeV Si ions. The abscissa axis is converted from fluence to dpa. The photosensitivity of the undoped a-Si:H, which was above 10^5 before irradiation, decreased with increasing ion fluence and eventually became 1 at 5×10^{-4} dpa. On the other

hand, the photosensitivity of the p-type and n-type a-Si:Hs, which were 3.6 and 1.4 before irradiation respectively, slightly increased with increasing 2.8 MeV Si ion fluence and had a peak at 2×10^{-5} dpa. The peak value was around 9 in both cases. Since the ratio of decrease in PC was lower than that in DC, in other words, the ratio of decrease in carrier lifetime was lower than the ratio of decrease in dark majority carrier concentration due to the carrier removal effect, the increase in photosensitivity appeared. However, the values of photosensitivity decreased at above 2×10^{-5} dpa and became 1 at 5×10^{-4} dpa as was the case with the undoped a-Si:H. Since the electric conduction was dominated by the hopping transport at above 5×10^{-4} dpa, photo-excited carriers could not be transferred by the band conduction and no photoconduction appeared in this fluence regime.

It can be concluded from these results that a physical application limit for a-Si:H photoelectric devices in radiation environments is 5×10^{-4} dpa. However, the application limit fluence will be higher at higher temperature conditions when considering that the radiation damage in a-Si:H can thermally recover even at RT (see Fig. 7).

C. Hydrogen Bonding State Change Due to Self-Ion Irradiation

As mentioned in Section IV-A, the dominant electronic transport mechanism changes from the band conduction to the hopping conduction in the fluence regime of around 10^{-4} dpa, and its transition is based on the drastic increase in localized states between the mobility edges. Here, variation of the hydrogen concentration due to ion irradiation is discussed for the purpose of considering the possibility of the increase in hopping transport due to dehydrogenation.

Hydrogen-free a-Si has a very high dangling bond density (above 10^{20} cm^{-3}) and the electric conduction is mainly dominated by the hopping transport of carriers via localized states. However, hydrogenation results in the drastic decrease in dangling bond density (less than 10^{16} cm^{-3}), since hydrogen atoms terminate the dangling bonds in a-Si. The decrease in dangling bond density provides the decrease in hopping transport and the increase in band transport. Consequently, hydrogen atoms are an essential element for a-Si:H semiconductors and the hydrogen concentration strongly affects the electrical properties. Hence, if ion irradiation induces the hydrogen emission from the surface and the decrease in hydrogen concentration, the dominant conduction mechanism may change from the band transport to the hopping transport. Since most of hydrogen atoms in a-Si:H are bonded to Si atoms [38], the hydrogen concentration is correlated with the infrared absorption due to Si-H vibrations. The variations of hydrogen concentration and the bonding state due to ion irradiation was investigated using the Fourier transform infrared spectroscopy (FTIR). The samples were undoped a-Si:H films which were formed on double-polished c-Si substrates. The film thickness was 0.30 μm and the deposition condition was the same as that described in Section II.

A typical infrared absorption spectrum of device grade a-Si:H has two hydrogen related absorption bands: the wagging-rocking mode at ~ 640 cm^{-1} and the stretching mode at 2000–2100 cm^{-1}, which are respectively named the vibrational modes involving H motions [39]. The absorption band of the stretching mode centered at $\sim$ 2000 cm^{-1} is attributed to isolated monohydrides, Si-H. The stretching mode centered at $\sim$ 2100 cm^{-1} is associated with the clustered monohydrides, $(\mathrm{Si-H})_n$ as well as polyhydrides, $\mathrm{Si-H_2}$ and $\mathrm{Si-H_3}$. Hereinafter, the former and the latter are represented as the isolated hydrogen and the clustered hydrogen, respectively. Each hydrogen concentration can be derived from the deconvolution of the stretching modes using the Gaussian function [40]. Assuming that the hydrogen concentration of a mode i is proportional to the integrated absorption I_i, the total hydrogen concentration C_{H} can be calculated as follows:

$$C_{\mathrm{H}} = \sum_i A_i \times I_i = \sum_i A_i \times \int \frac{\alpha_i(\omega)}{\omega} \mathrm{d}\omega \tag{6}$$

where ω and α represent the wavenumber (cm^{-1}) and the absorption coefficient (cm^{-1}), respectively. A_i is the proportionality factor (cm^{-2}). In this study, we used $A_{2000} = 6.8 \times 10^{19}$ cm^{-2} for the 2000 cm^{-1} mode and $A_{2100} = 2.0 \times 10^{20}$ cm^{-2} for the 2100 cm^{-1} mode, which were derived from the comparison of the integrated absorption to the absolute hydrogen concentration experimentally obtained from ERDA. These values are close to the values proposed by Amato *et al.* [41]. The absorption coefficient α was calculated by the method of Brodsky, Cardona, and Cuomo (BCC method) [42], [43]. In the BCC method, multiple reflections in both the front surface and the back surface of sample are considered, whereas the refection at the interface between a-Si:H film and c-Si substrate is ignored. Also, the refractive index of a-Si:H film is assumed to be the same as that of c-Si substrate. Then, the following relationship between the absorption coefficient, α and the transmittance of a-Si:H film, T is obtained:

$$\alpha(\omega) = \frac{1}{d}\left\{\ln(XR) - \ln(\sqrt{1-X^2}-1)\right\} \tag{7}$$

$$X = \frac{2R}{(1-R^2)T} \tag{8}$$

where d the film thickness (cm) and R an empirically determined interface multiple reflection loss. The value of T is derived from the following equation:

$$T = \frac{T_1}{T_2 \times T_{\mathrm{b}}} \tag{9}$$

where T_1, T_2, and T_{b} is the transmittance of sample, the transmittance of c-Si substrate, and the baseline correction to remove interference effects, respectively. The sum of a quartic function and a trigonometric function was used for $1/T_{\mathrm{b}}$ [44]. Assuming the absorption-free transmission of c-Si substrate, $T_2 = 0.54 = (1-R)/(1+R)$ and thus $R = 0.30$ are derived. Therefore, (7) can be rewritten as follows:

$$\alpha(\omega) = \frac{1}{d}\left\{\ln(0.196T) - \ln(\sqrt{1-0.43T^2}-1)\right\}. \tag{10}$$

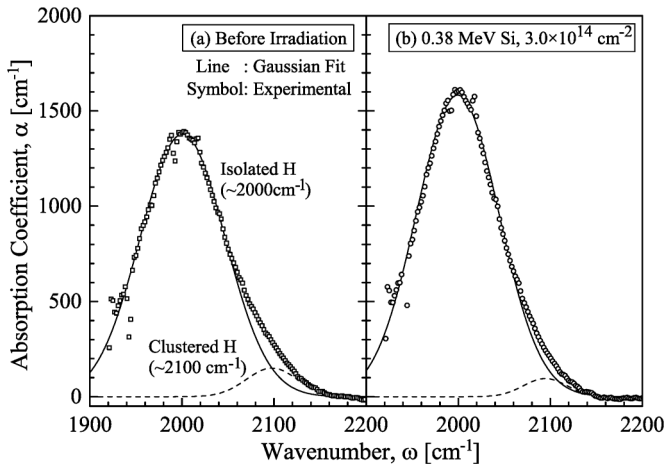

Fig. 13. Absorption coefficient for stretching modes in the undoped a-Si:H (a) before irradiation and (b) after irradiation with 0.38 MeV Si ions at 3.0×10^{14} cm^{-2}. Symbols are the experimental values. Solid and dashed lines denote the Gaussian peaks originating from the isolated hydrogen (2000 cm^{-1}) and the clustered hydrogen (2100 cm^{-1}), respectively.

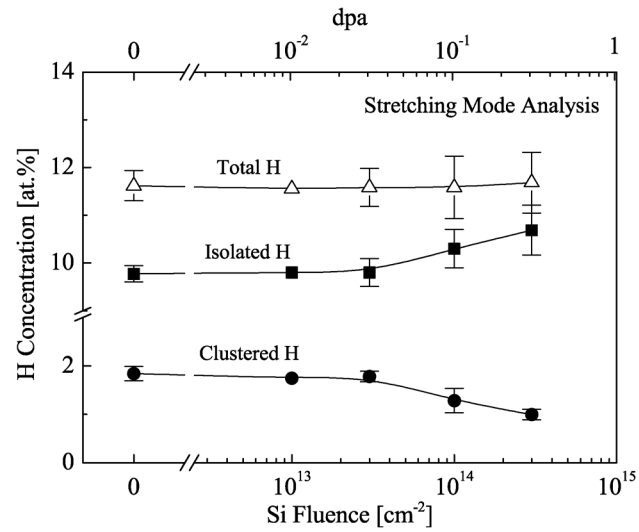

Fig. 14. Variations of the hydrogen concentration and the bonding state in the undoped a-Si:H due to 0.38 MeV Si ion irradiation. Closed squares and circles represent the concentrations of the isolated hydrogen and the clustered hydrogen which were derived from the integrated absorption of the stretching modes at 2000 cm^{-1} and 2100 cm^{-1}, respectively. Open triangles represent the total hydrogen concentration. Solid lines are introduced to guide the eye. The same is true in Fig. 15.

However, it is known that a large error is included in the relatively low wavenumber and it can be corrected by the following equation:

$$\alpha(\omega) = \begin{cases} \frac{\alpha_{\mathrm{BCC}}}{(1.72-12\omega\, d)} & \omega\, d < 0.06 \\ \alpha_{\mathrm{BCC}} & \omega\, d \geq 0.06 \end{cases}. \tag{11}$$

The absorption coefficient in (7) and (10), $\alpha(\omega)$ is rewritten to "α_{BCC}" in (11). The error in absorption coefficient is usually less than 10% [43].

Fig. 13 shows variation of the absorption coefficient for the stretching modes due to 0.38 MeV Si ion irradiation at the fluence of 3.0×10^{14} cm^{-2}. The broad absorption peak appeared between 1900 cm^{-1} and 2200 cm^{-1} could be deconvoluted into two peaks by the Gaussian function (the solid and dotted lines in Fig. 13): the strong absorption peak centered at 2000 cm^{-1} and the relatively weak absorption peak centered at 2100 cm^{-1}. Hence, most of bonded hydrogen atoms were isolated and a little was clustered, indicating that the quality of the samples were high (that is, "device-grade"), since the clustered hydrogen is widely believed to deteriorate the photoelectric properties [31], [45]. It was derived from the absorption spectrum in Fig. 13(a) and (6) that the isolated hydrogen concentration before irradiation was 9.8 at.% and the clustered one was 1.8 at.%. The hydrogen concentration (at.%) was calculated by using 4.9×10^{22} cm^{-3} for Si atomic concentration in the a-Si:H. After irradiation with 0.38 MeV Si ions, the increase in absorption peak at 2000 cm^{-1} and the decrease in absorption peak 2100 cm^{-1} were observed. The results also showed that the isolated hydrogen increased to 10.7 at.% and the clustered hydrogen decreased to 1.0 at.%. This is thought to be due to the "mixing effect" of ion irradiation. That is, the clustered hydrogen atoms were dispersed (intermixed) because of a significant atomic rearrangement by energetic ions, and as a result, they were isolated [46].

Fig. 14 shows variations of the hydrogen concentration in the undoped a-Si:H due to 0.38 MeV Si ion irradiation. The isolated hydrogen concentration increased and the clustered hydrogen concentration decreased with increasing fluence although the sum of them was constant. This result indicates that the clustered hydrogen atoms were isolated by the mixing effect and the total hydrogen concentration did not change up to 0.31 dpa. Here, it should be noted that the recovery effect was expected to be included somewhat in these results, since the FTIR measurement was not performed *in-situ*. As shown in Figs. 6 and 7, radiation effects can be reversed with time after irradiation at RT. Therefore, when taking into account the recovery effect, a part of the hydrogen atoms isolated due to irradiation were possibly clustered again and the mixing effect might be underestimated. However, the total hydrogen concentration was not affected by the recovery effect after irradiation. If the hydrogen atoms or molecules were released from the surface, and as a result, the total hydrogen concentration decreased, the total hydrogen concentration would never be reversed by the annealing effect.

Fig. 15 shows variations of the hydrogen concentration in the undoped a-Si:H due to 0.20 MeV H_2 ion irradiation. One H_2 ion with energy of 0.20 MeV is equivalent to two protons with energies of 0.10 MeV and the same radiation effect was expected. In this case, most of 0.20 MeV H_2 ions were implanted in the c-Si substrate and the total hydrogen concentration increased with increasing fluence. Assuming that the implanted hydrogen atoms were contained in the a-Si:H film, the apparent increase in hydrogen concentration due to the implanted hydrogen atoms could be derived (Gray triangles in Fig. 15). The increase in total hydrogen concentration was in good agreement with the increase in the implanted hydrogen atoms. This result indicates that the increase in total hydrogen concentration at the fluence above 1.0×10^{16} H/cm^2 was caused by the implanted hydrogen atoms. However, the clustered hydrogen concentration (closed circles) decreased from 1.8 to 1.4 at.% at the fluence of 3.0×10^{16} cm^{-2} (6.7×10^{-3} dpa) and increased at 1.0×10^{17} cm^{-2} (2.2×10^{-2} dpa) although the isolated hydrogen concentration

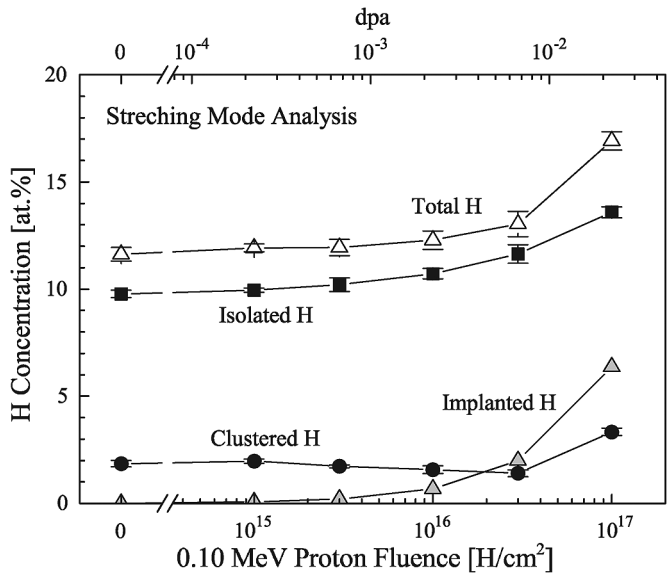

Fig. 15. Variations of the hydrogen concentration and the bonding state in the undoped a-Si:H due to 0.20 MeV H_2 ion irradiation. Note that the abscissa axis in the lower part represents the fluence of irradiated hydrogen atoms, not the number of H_2 ions. Gray triangles represent the apparent implanted-H concentration when assuming that the implanted hydrogen atoms are contained within the a-Si:H film.

constantly increased with increasing the fluence. This is thought to be because the implanted hydrogen atoms were clustered in the high fluence regime (around 10^{17} cm^{-2}), whereas the clustered hydrogen atoms in the a-Si:H film were isolated by the mixing effect of ion irradiation, as is the case in Fig. 14.

When comparing the results of Fig. 4 with Fig. 15, it is found that the increase in DC based on the increase in the hopping transport arose at the fluence above 1.0×10^{14} cm^{-2} (2.2×10^{-5} dpa) although no change in the hydrogen bonding state was produced in that fluence regime. In addition, no decrease in hydrogen concentration due to ion irradiation was detected in the fluence regime investigated in this study. This fact was also confirmed by ERDA. Therefore, it is concluded that the transition from the band conduction to the hopping conduction is caused by the large accumulation of dangling bonds and also the transition of electric conduction occurs in the fluence regime of around 10^{-4} dpa. It has also been reported that DC of hydrogen-free a-Si irradiated with MeV-Si ions increased with increasing the fluence and the increase in DC was attributed to the increase in the hopping transport accompanied by the accumulation of dangling bonds [11]. This fact suggests that the similar DC variations occurs in a-Si and a-Si:H regardless of hydrogenation in the high fluence regime despite that the hydrogenation play a crucial role in passivating the dangling bonds.

V. Conclusion

Electric conductivity variations of a-Si:H due to self-ion irradiation as functions of ion species, ion energy, and irradiation fluence were investigated in detail. As a result, the comprehensive and systematic interpretation as for the conductivity variations was successfully obtained.

From the results of 10 MeV proton and 0.10 MeV proton irradiations, it was shown that DC and PC of the undoped a-Si:H increased with increasing the proton fluence in the low fluence regime, and had a peak at around 7×10^{20} eV/cm^3. It was also shown from the Seebeck effect analysis that the increase in DC and PC was attributed to donor-center generation via the electronic excitation effect of incident protons. This conclusion is in consistent with the report by Kishimoto *et al.* [12]. However, further irradiation induces the decrease in DC and PC because of accumulation of dangling bonds, which result in both the carrier removal effect and the decrease in carrier lifetime. Furthermore, it was found from the results of 0.10 MeV proton irradiation and 2.8 MeV Si ion irradiation that only the DC increased with increasing the fluence in the high fluence regime above 10^{-4} dpa, whereas the photoconduction was lost. This indicates that the dominant electric conduction mechanism changes from the band transport to the hopping transport due to the excessive accumulation of dangling bonds. This conclusion is in consistent with the report by Coffa *et al.* [11]. The increase in DC due to enhancement of the hopping transport is independent of the majority carrier concentration before irradiation and the hydrogenation which provide the decrease in the dangling bond density. In addition to the increase in hopping site density, the increase in hopping mobility may contribute the enhancement of hopping transport. The accumulation of dgangling bonds is mainly caused by the displacement damage effect. These conductivity variations due to self-ion irradiation, which include both the anomalous enhancement and the transition from the band transport to the hopping transport, can be systematically categorized according to the ratio of the nuclear energy deposition to the electronic energy deposition of incident ions. Additionally, both the donor-centers appeared in the low fluence regime and the dangling bonds accumulated in the high fluence regime are metastable at RT and gradually decay with time.

Acknowledgment

The authors would like to thank Dr. Hitoshi Sai and Dr. Michio Kondo of National Institute of Advanced Industrial Science and Technology (AIST) for fabricating the a-Si:H samples. We also would like to thank Dr. Kazunori Shimazaki and Dr. Mitsuru Imaizumi of Japan Aerospace Exploration Agency (JAXA) for their technical support.

References

[1] A. Holmes-Siedle and L. Adams, *Handbook of Radiation Effects 2nd ed.*. Oxford, U.K.: Oxford Univ. Press, 2007.

[2] R. Velazco, P. Fouillat, and R. Reis, *Radiation Effects on Embedded Systems*. Dordrecht, The Netherlands: Springer, 2007.

[3] P. J. Sellin and J. Vaitkus, "New materials for radiation hard semiconductor detectors," *Nucl. Instrum. Meth. A*, vol. 557, pp. 479–489, 2006.

[4] N. Wyrsch, C. Miazza, S. Dunand, C. Ballif, A. Shah, M. Despeisse, D. Moraes, F. Powolny, and P. Jarron, "Radiation hardness of amorphous silicon particle sensors," *J. Non-Cryst. Solids*, vol. 352, pp. 1797–1800, 2006.

[5] N. Kishimoto, H. Amekura, K. Kono, and C. G. Lee, "Radiation resistance of amorphous silicon in optoelectric properties under proton bombardment," *J. Nucl. Mater.*, vol. 258-263, pp. 1908–1913, 1998.

[6] E. Morgado, R. Schwarz, T. Braz, C. Casteleiro, A. Maçarico, M. Vieira, and E. Alves, "Radiation-induced defects in a-Si:H by 1.5 MeV He4 particles studied by photoconductivity and photothermal deflection spectroscopy," *J. Non-Cryst. Solids*, vol. 352, pp. 1071–1074, 2006.

[7] P. Danesh, B. Pantchev, and E. Vlaikova, "18 MeV electron irradiation-induced metastability in hydrogenated amorphous silicon," *Nucl. Instrum. Meth. B*, vol. 239, pp. 370–374, 2005.

[8] A. Scholz and B. Schröder, "Interpretation of the saturation behavior of the metastable defect density created in intrinsic a-Si:H by keV-electron irradiation," *J. Non-Cryst. Solids*, vol. 137&138, pp. 259–262, 1991.

[9] S. Gangopadhyay, B. Schröder, and J. Geiger, "The density of states of sputtered a-Si: H studied by the space-charge-limited current technique: The influence of deposition parameters, light and keV electron irradiation," *Philos. Mag. B*, vol. 56, pp. 321–333, 1987.

[10] J. R. Srour, J. W. Palko, D. H. Lo, S. H. Liu, R. L. Mueller, and J. C. Nocerino, "Radiation effects and annealing studies on amorphous silicon solar cells," *IEEE Trans. Nucl. Sci.*, vol. 56, no. 6, pp. 3300–3306, Dec. 2009.

[11] S. Coffa, F. Priolo, and A. Battaglia, "Defect production and annealing in ion-implanted amorphous silicon," *Phys. Rev. Lett.*, vol. 70, pp. 3756–3579, 1993.

[12] N. Kishimoto, H. Amekura, K. Kono, and C. G. Lee, "Stable photoconductivity in metastable a-Si:H under high-energy proton irradiation," *J. Non-Cryst. Solids*, vol. 227–230, pp. 238–242, 1998.

[13] J. J. Loferski and P. Rappaport, "Radiation damage in Ge and Si detected by carrier lifetime: Damage thresholds," *Phys. Rev.*, vol. 111, pp. 432–439, 1958.

[14] H. Amekura, N. Kishimoto, and K. Kono, "Radiation-induced tow-step degradation of Si photoconductors and space solar cells," *IEEE Trans. Nucl. Sci.*, vol. 45, no. 3, pp. 1508–1513, Jun. 1998.

[15] M. Levalois, J. P. Girard, G. Allais, A. Hairie, M. N. Metzner, and E. Paumier, "High energy ion irradiation of germanium," *Nucl. Instrum. Meth. B*, vol. 63, pp. 25–29, 1992.

[16] H. Matsuura, H. Iwata, S. Kagamihara, R. Ishihara, M. Komeda, H. Imai, M. Kikuta, Y. Inoue, T. Hisamatsu, S. Kawakita, T. Ohshima, and H. Itoh, "Si substrate suitable for radiation-resistant space solar cells," *Jpn. J. Appl. Phys.*, vol. 45, pp. 2648–2655, 2006.

[17] S. Sato, H. Sai, T. Ohshima, M. Imaizumi, K. Shimazaki, and M. Kondo, "Electric properties of undoped hydrogenated amorphous silicon semiconductors irradiated with self-ions," *Nucl. Instrum. Meth. B*, vol. 285, pp. 107–111, 2012.

[18] S. Sato, H. Sai, T. Ohshima, M. Imaizumi, K. Shimazaki, and M. Kondo, "Temporal electric conductivity variations of hydrogenated amorphous silicon due to high energy protons," *J. Non-Cryst. Solids*, vol. 358, pp. 2039–2043, 2012.

[19] S. Sato, H. Sai, T. Ohshima, M. Imaizumi, K. Shimazaki, and M. Kondo, "Proton-induced photoconductivity increment and the thermal stability of a-Si:H thin film," *J. Non-Cryst. Solids*, vol. 356, pp. 2114–2119, 2010.

[20] S. Sato, H. Sai, T. Ohshima, M. Imaizumi, K. Shimazaki, and M. Kondo, "Anomalous enhancement in radiation induced conductivity of hydrogenated amorphous silicon semiconductors," *Nucl. Instrum. Meth. B*, vol. 286, pp. 29–34, 2012.

[21] [Online]. Available: http://www.srim.org/

[22] S. Sato, H. Sai, T. Ohshima, M. Imaizumi, K. Shimazaki, and M. Kondo, "Temporal donor generation in undoped amorphous silicon induced by swift proton bombardment," *Appl. Phys. Express*, vol. 4, p. 061401, 2011.

[23] C. E. Nebel and R. A. Street, "High field transport in a-Si:H," *Int. J. Mod. Phys. B*, vol. 7, pp. 1207–1258, 1993.

[24] C. E. Nebel and R. A. Street, "Space-charge-limited-currents at low temperatures in hydrogenated amorphous silicon," *Philos. Mag. B*, vol. 67, pp. 721–731, 1993.

[25] R. Stachowitz, W. Fuhs, and K. Johndr, "Low-temperature tranport and recombination in a-Si:H," *Philos. Mag. B*, vol. 62, pp. 5–18, 1990.

[26] D. Redfield and R. H. Bube, "Reinterpretation of degradation kinetics of amorphous silicon," *Appl. Phys. Lett.*, vol. 54, pp. 1037–1039, 1989.

[27] A. Khan, M. Yamaguchi, J. C. Bourgoin, and T. Takamoto, "Thermal annealing study of 1 MeV electron-irradiation-induced defects in n^+p InGaP diodes and solar cells," *J. Appl. Phys.*, vol. 91, pp. 2391–2397, 2002.

[28] D. A. Anderson and W. E. Spear, "Photoconductivity and recombination in doped amorphous silicon," *Philos. Mag.*, vol. 36, pp. 695–712, 1977.

[29] O. Astakhov, F. Finger, R. Carius, A. Lambertz, Y. Petrusenko, V. Borysenko, and D. Barankov, "Electron spin resonance studies of microcrystalline and amorphous silicon irradiated with high energy electrons," *J. Non-Cryst. Solids*, vol. 352, pp. 1020–1023, 2006.

[30] P. G. Le Comber and W. E. Spear, "Electronic transport in amorphous silicon films," *Phys. Rev. Lett.*, vol. 25, pp. 509–511, 1970.

[31] N. F. Mott and E. A. Davis, *Electronic Processes in Non-Crystalline Materials*. Oxford, U.K.: Oxford Univ. Press, 1979.

[32] H. Dersch, A. Skumanich, and N. M. Amer, "Influence of dangling-bond defects on recombination in a-Si:H," *Phys. Rev. B*, vol. 31, pp. 6913–6916, 1985.

[33] H. Stitzl, G. Krötz, and G. Müller, "Accumulation and annealing of implantation damage in a-Si:H," *Appl. Phys. A*, vol. 53, pp. 235–240, 1991.

[34] C. Cloude, W. E. Spear, P. G. Le Comber, and A. C. Hourd, "Low-temperature electron transport near the mobility edge of amorphous silicon," *Philos. Mag. B*, vol. 54, pp. L113–L118, 1986.

[35] J. Kočka, O. Klíma, E. Šipek, C. E. Nebel, G. H. Bauer, G. Juška, and M. Hoheisel, "a-Si:H electron drift mobility measured under extremely high electric field," *Phys. Rev. B*, vol. 45, pp. 6593–6600, 1992.

[36] C. E. Nebel, "Transport in a-Si:H," *J. Non-Cryst. Solids*, vol. 137&138, pp. 395–400, 1991.

[37] P. G. Le Comber, A. Madan, and W. E Spear, "Electronic transport and state distribution in amorphous Si films," *J. Non-Cryst. Solids*, vol. 11, pp. 219–234, 1972.

[38] J. B. Boyce and M. Stutzmann, "Orientation ordering and melting of molecular H_2 in an a-Si Matrix: NMR studies," *Phys. Rev. Lett.*, vol. 54, pp. 562–565, 1985.

[39] G. Lucovsky, R. J. Nemanich, and J. C. Knights, "Structural interpretation of the vibrational spectra of a-Si:H alloys," *Phys. Rev. B*, vol. 19, pp. 2064–2073, 1979.

[40] H. Shanks, C. J. Fang, L. Ley, M. Cardona, F. J. Demond, and S. Kalbitzer, "Infrared spectrum and structure of hydrogenated amorphous silicon," *Phys. Stat. Sol. (b)*, vol. 100, pp. 43–55, 1980.

[41] G. Amato, G. Della Mea, F. Fizzotti, C. Manfredotti, R. Marchisio, and A. Paccagnella, "Hydrogen bonding in amorphous silicon with use of low-pressure chemical-vapor-deposition technique," *Phys. Rev. B*, vol. 43, pp. 6627–6633, 1991.

[42] M. H. Brodsky, M. Cardona, and J. J. Cuomo, "Infrared and Raman spectra of the silicon-hydrogen bonds in amorphous silicon prepared by glow discharge and sputtering," *Phys. Rev. B*, vol. 16, pp. 3556–3571, 1977.

[43] N. Maley, "Critical investigation of the infrared-transmission-data analysis of hydrogenated amorphous silicon alloys," *Phys. Rev. B*, vol. 46, pp. 2078–2085, 1992.

[44] C. Manfredotti, F. Fizzotti, M. Boero, P. Pastorino, P. Polesello, and E. Vittone, "Influence of hydrogen-bonding configurations on the physical properties of hydrogenated amorphous silicon," *Phys. Rev. B*, vol. 50, pp. 18046–18053, 1994.

[45] J. Daey Ouwens, R. E. I. Schropp, and W. F. van der Weg, "Interpretation of the silicon-hydrogen stretching doublet in a-Si:H hydrogenated amorphous silicon," *Appl. Phys. Lett.*, vol. 65, pp. 204–206, 1994.

[46] M. Nastasi, J. W. Mayer, and J. K. Hirovonen, *Ion-Solid Interactions: Fundamentals and Applications*. Cambridge, U.K.: Cambridge Univ. Press, 1996, ch. 11, p. 295.